


Measurement of the Groomed Jet Radius and Momentum Splitting Fraction in pp and Pb-Pb Collisions at $\sqrt{s_{NN}} = 5.02$ TeV

S. Acharya *et al.**

A Large Ion Collider Experiment Collaboration

 (Received 25 August 2021; revised 29 November 2021; accepted 10 February 2022; published 7 March 2022)

This article presents groomed jet substructure measurements in pp and Pb-Pb collisions at $\sqrt{s_{NN}} = 5.02$ TeV with the ALICE detector. The soft drop grooming algorithm provides access to the hard parton splittings inside a jet by removing soft wide-angle radiation. We report the groomed jet momentum splitting fraction, z_g , and the (scaled) groomed jet radius, θ_g . Charged-particle jets are reconstructed at midrapidity using the anti- k_T algorithm with resolution parameters $R = 0.2$ and $R = 0.4$. In heavy-ion collisions, the large underlying event poses a challenge for the reconstruction of groomed jet observables, since fluctuations in the background can cause groomed parton splittings to be misidentified. By using strong grooming conditions to reduce this background, we report these observables fully corrected for detector effects and background fluctuations for the first time. A narrowing of the θ_g distribution in Pb-Pb collisions compared to pp collisions is seen, which provides direct evidence of the modification of the angular structure of jets in the quark-gluon plasma. No significant modification of the z_g distribution in Pb-Pb collisions compared to pp collisions is observed. These results are compared with a variety of theoretical models of jet quenching, and provide constraints on jet energy-loss mechanisms and coherence effects in the quark-gluon plasma.

DOI: [10.1103/PhysRevLett.128.102001](https://doi.org/10.1103/PhysRevLett.128.102001)

Introduction.—Ultrarelativistic heavy-ion collisions at the Large Hadron Collider (LHC) are used to study the high temperature deconfined phase of strongly interacting matter known as the quark-gluon plasma (QGP) [1–5]. Highly energetic jets created early in the collisions interact with the QGP medium and through those interactions they can lose energy and their internal structure can be modified. This process, known as jet quenching, can be used to reveal the physical properties of the QGP itself such as its transport coefficients and the quasiparticle nature of its degrees of freedom as a function of scale [6–9]. Experimentally, jet quenching is evaluated by comparing jet measurements in heavy-ion collisions to analogous measurements in pp collisions [10–18]. Notably, measurements of the jet angularity [16] and jet transverse profile [18], which are sensitive to a combination of the angular and momentum space structure of jets, suggest a narrowing of the jet core in heavy-ion collisions. Nonetheless, up to now, no direct modification of the intrajet angular distribution alone has been measured.

Jet grooming algorithms provide access to the hard (high-momentum transfer) parton splittings inside a jet by removing soft wide-angle radiation [19–21]. Access to the hard splittings isolates substructures that are well-controlled in perturbative QCD (pQCD), which in heavy-ion collisions may help constrain various jet quenching effects such as energy loss, transverse-momentum broadening, and color coherence. Measurements of groomed jet observables in heavy-ion collisions have been performed by the ALICE and CMS Collaborations [22–24], and opened a new avenue in the study of jet substructure in heavy-ion collisions.

The soft drop (SD) [19–21] grooming algorithm identifies a single splitting by first reconstructing a jet with the anti- k_T algorithm and then reclustering the constituents of the jet using the Cambridge-Aachen (CA) algorithm [25] in order to follow the angular ordering of the QCD parton shower. The splitting is selected from within the history of the reclustering with a grooming condition, $z > z_{\text{cut}}\theta^\beta$, where β and z_{cut} are tunable parameters, z is the fraction of transverse momentum (p_T) carried by the subleading (lowest p_T) prong,

$$z \equiv \frac{p_{T,\text{subleading}}}{p_{T,\text{leading}} + p_{T,\text{subleading}}}, \quad (1)$$

and θ is the relative angular distance between the leading and subleading prong,

*Full author list given at the end of the article.

Published by the American Physical Society under the terms of the [Creative Commons Attribution 4.0 International license](https://creativecommons.org/licenses/by/4.0/). Further distribution of this work must maintain attribution to the author(s) and the published article's title, journal citation, and DOI.

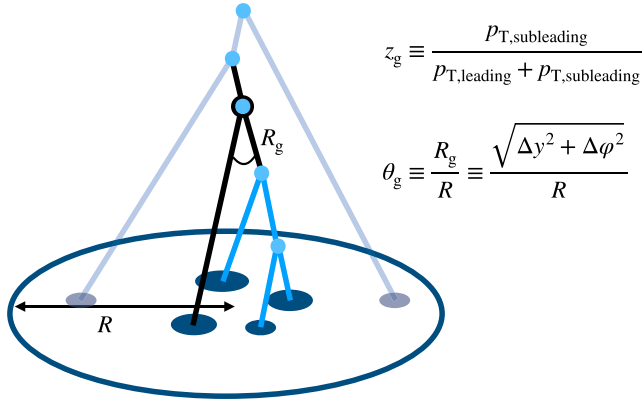


FIG. 1. Graphical representation of the angularly ordered Cambridge-Aachen reclustering of jet constituents and subsequent soft drop grooming procedure [19], with the identified splitting denoted in black and the splittings that were groomed away in light blue.

$$\theta \equiv \frac{\sqrt{\Delta y^2 + \Delta \phi^2}}{R}, \quad (2)$$

where Δy and $\Delta \phi$ are the distances measured in rapidity and azimuthal angle, respectively, and R is the jet resolution parameter. The groomed splitting is then characterized by two relevant kinematic observables: the groomed momentum fraction, z_g , and the (scaled) groomed jet radius, θ_g , which are the values of z and θ of Eqs. (1) and (2) for the identified splitting, as shown in Fig. 1.

In pp collisions, measurements of the θ_g and z_g distributions were performed at RHIC and the LHC [23,26–29]. At high-transverse momentum p_T , the data are described within uncertainties by PQCD predictions [30].

In heavy-ion collisions, it was proposed that θ_g may be sensitive to several important jet-quenching physics mechanisms: the relative suppression of gluon vs quark jets, transverse-momentum broadening, and the ability of the medium to resolve a color dipole as two independent color charges [31,32]. Uncertainty principle arguments suggest that wider splittings are formed earlier in vacuum than narrower splittings ($t_f \sim 1/\theta_g^2$ where t_f is the splitting formation time). In heavy-ion collisions, this would result in wider splittings traversing a longer path in the medium on average. Complementary to θ_g , it has been argued that z_g may be sensitive to the modification of the Dokshitzer-Gribov-Lipatov-Altarelli-Parisi splitting function in the QGP, the breaking of color coherence, and the response of the medium to the jet [33–36]. By measuring both θ_g and z_g simultaneously, and thereby both the angular and momentum scales of the hard substructure of jets, these jet quenching mechanisms can be further constrained.

Up to now, no measurement of θ_g has been performed in heavy-ion collisions. Previous measurements of the z_g distribution by the CMS [22] and ALICE Collaborations

[23] indicated significant modification with respect to pp collisions. However, these results were not corrected for background and detector effects, and are difficult to compare directly to theoretical calculations [37]. In this Letter, we report the first fully corrected measurement of groomed substructure observables in heavy-ion collisions, allowing for a rigorous comparison with theoretical calculations.

Experimental setup and datasets.—A description of the ALICE detector and its performance can be found in Refs. [38,39]. The pp data set used in this analysis was collected in 2017 during LHC Run 2 at $\sqrt{s} = 5.02$ TeV using a minimum-bias (MB) trigger defined by the coincidence of the signals from two scintillator arrays in the forward region (V0 detectors) [40]. The Pb-Pb dataset was collected in 2018 at $\sqrt{s_{NN}} = 5.02$ TeV. Central and semi-central triggers that select events in the 0%–10% and 30%–50% centrality intervals based on the multiplicity of produced particles in the forward V0 detectors, were used [41,42]. The event selection includes a primary-vertex selection and the removal of beam-induced background events and pileup [10]. After these selections, the pp data sample contains 870 million events and corresponds to an integrated luminosity of $18.0 \pm 0.4 \text{ nb}^{-1}$ [43]. The Pb-Pb data sample contains 92 million events in central collisions and 90 million events in semicentral collisions, corresponding to an integrated luminosity of 0.12 nb^{-1} and 0.06 nb^{-1} , respectively.

This analysis uses charged-particle tracks reconstructed using information from both the Time Projection Chamber (TPC) [44] and the Inner Tracking System (ITS) [45]. While track-based observables are collinear unsafe [46–48], they can be measured with greater precision than calorimeter-based observables and recent measurements have demonstrated that for the groomed jet observables considered here, track-based distributions are compatible with the corresponding collinear-safe distributions [49]. Tracks with $0.15 < p_T < 100 \text{ GeV}/c$ were accepted over pseudorapidity range $|\eta| < 0.9$. Further details about the track selection are described in Ref. [50]. The accepted tracks exhibit approximately uniform azimuthal acceptance and momentum resolution $\sigma(p_T)/p_T$ ranging from about 1% at track $p_T = 1 \text{ GeV}/c$ to 4% at track $p_T = 50 \text{ GeV}/c$.

Analysis method.—Jets were reconstructed from charged-particle tracks with FastJet3.2.1 [51] using the anti- k_T algorithm with E -scheme recombination for resolution parameters $R = 0.2$ and 0.4 [52,53]. The pion mass is assumed for all jet constituents. Jets in heavy-ion collisions have a large uncorrelated background contribution due to fluctuations in the underlying event (UE) [54]. The event-by-event constituent subtraction method was used, which corrects the overall jet p_T and its substructure simultaneously by subtracting UE energy constituent by constituent [55,56]. A maximum recombination distance

$R_{\max} = 0.25$ was used. After background subtraction, the measured range is $40 < p_{T,\text{chjet}} < 120$ GeV/ c . The jet axis is required to be within the fiducial volume of the TPC, $|\eta_{\text{jet}}| < 0.9 - R$, where η_{jet} is the jet pseudorapidity.

Local background fluctuations in a heavy-ion collision environment can result in an incorrect splitting (unrelated to the hard scattering) being identified by the grooming algorithm. In order to address this issue, the measurement was performed by applying a strong grooming condition, $z_{\text{cut}} = 0.2$ (with $\beta = 0$), which better mitigates these effects as compared to softer grooming conditions (e.g., $z_{\text{cut}} = 0.1$) [37]. To further reduce the mistagging effects, we report measurements with either a small resolution parameter ($R = 0.2$ in central collisions) or with more peripheral collisions (30%–50% for $R = 0.4$).

The rate of prong mistagging from residual background effects was evaluated by embedding jets simulated with the PYTHIA8 event generator [57] into measured Pb-Pb data and following the procedure in Ref. [37]. The residual background contribution ranges from approximately 5% up to 15% at lower p_T , in more central events, and at larger R . This level of background contamination is small enough to allow the results to be unfolded for detector effects and background fluctuations. The impact of the residual background contribution remains one of the main sources of systematic uncertainty [50].

The reconstructed $p_{T,\text{chjet}}$, θ_g , and z_g distributions were corrected for effects related to the tracking inefficiency, particle-material interactions, and track p_T resolution. Moreover, in Pb-Pb collisions, background fluctuations significantly smear the reconstructed distributions of θ_g and z_g . To account for these effects, events were simulated with the PYTHIA8 generator using the Monash 2013 tune [57] and the GEANT3 model [58] for the particle transport in the ALICE detectors' material. For the Pb-Pb data, we embedded the simulated events into measured Pb-Pb data to mimic the background effects. A four-dimensional response matrix describing the detector and background response in $p_{T,\text{chjet}}$ and θ_g or z_g was constructed and used in the two-dimensional unfolding in $p_{T,\text{chjet}}$, θ_g , or z_g using the iterative Bayesian unfolding algorithm [59,60].

Systematic uncertainties.—The largest systematic uncertainties in this measurement originate from the tracking inefficiency, the unfolding procedure, residual mistagged prongs, and the background subtraction procedure. The total systematic uncertainty is calculated as the quadratic sum of all of the individual systematic uncertainties described below.

The systematic uncertainty due to the uncertainty of the tracking efficiency is evaluated using random rejection of additional tracks in jet finding according to the estimated tracking efficiency uncertainty of 4%, based on variations in the track selection criteria and on the ITS-TPC track-matching efficiency uncertainty. The systematic uncertainty arising from the unfolding regularization procedure is

evaluated by varying the number of unfolding iterations by ± 2 units, scaling the prior distribution, varying the binning, and varying the lower bound in the detector-level charged-particle jet transverse momentum $p_{T,\text{det}}^{\text{chjet}}$ range by 5 GeV/ c . The systematic uncertainty due to the model-dependence of the generator used to construct the response matrix is estimated by comparing results obtained with PYTHIA [57], HERWIG [61], and JEWEL [62]. The systematic uncertainty due to the bias introduced by the constituent subtraction procedure is estimated by varying R_{\max} from “undersubtraction” ($R_{\max} = 0.05$) to “oversubtraction” ($R_{\max} = 0.7$), around the nominal value of $R_{\max} = 0.25$. The systematic uncertainty due to a possible residual contamination of mistagged splittings after unfolding is estimated with a closure test. The total relative systematic uncertainty ranges from 3%–24% for θ_g and 4%–10% for z_g . See Ref. [50] for more details about the systematic uncertainties used in this measurement.

Results.—We report the θ_g and z_g distributions in the $p_{T,\text{chjet}}$ interval between 60 and 80 GeV/ c for $z_{\text{cut}} = 0.2$ in central (0%–10%, $R = 0.2$) and semicentral (30%–50%, $R = 0.4$) Pb-Pb collisions. The distributions are reported as normalized differential cross sections,

$$\frac{1}{\sigma_{\text{jet,inc}}} \frac{d\sigma}{dz_g} = \frac{1}{N_{\text{jet,inc}}} \frac{dN}{dz_g}, \quad (3)$$

where N is the number of jets passing the SD condition with a given $p_{T,\text{chjet}}$, $N_{\text{jet,inc}}$ is the number of inclusive jets, and $\sigma, \sigma_{\text{jet,inc}}$ are the corresponding cross sections. The analog of Eq. (3) also applies for θ_g .

The z_g and θ_g distributions are shown in Figs. 2 and 3, respectively. The distributions from Pb-Pb collisions are compared with the corresponding distributions from pp collisions, with their ratios displayed in the bottom panels. The relative uncertainties are assumed to be uncorrelated between pp and Pb-Pb collisions, and are added in quadrature in the ratio. In Pb-Pb collisions the precision of the measurements decreases as the jet resolution parameter is increased or the centrality is decreased, as the prong mistagging probability decreases with centrality and with decreasing R .

The fraction of jets that do not contain a splitting which passes the SD condition (f_{tagged}) differs by at most 1% between Pb-Pb and pp collisions. Therefore, any modifications in Pb-Pb compared to pp collisions can change the shape of the distribution, but keep the integral approximately the same.

The z_g distributions in Pb-Pb and pp collisions are consistent within experimental uncertainties for all jet momenta, jet resolution parameters, and centralities measured.

The situation is remarkably different when comparing the groomed jet radius, θ_g , in both systems. For $R = 0.2$ in

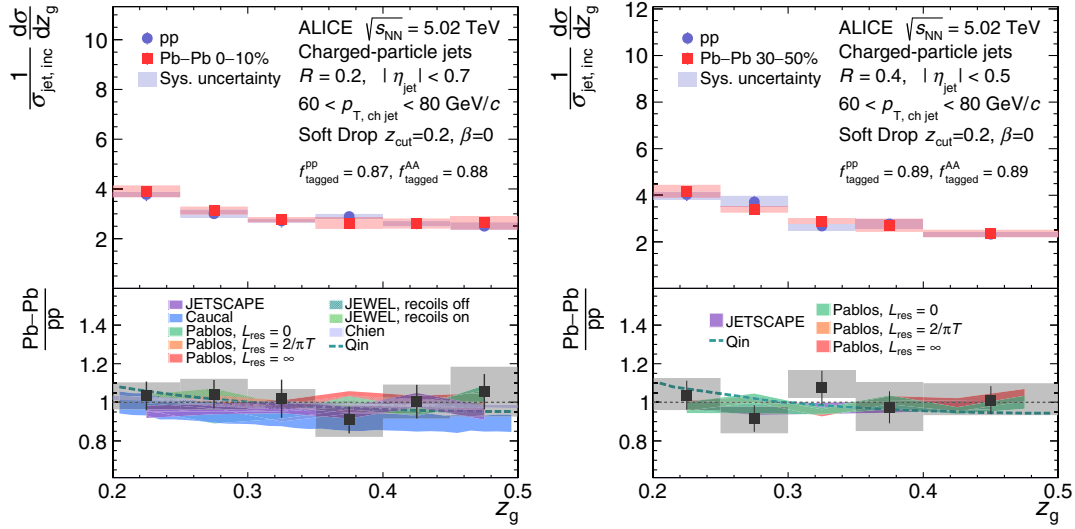


FIG. 2. Unfolded z_g distributions for charged-particle jets in pp collisions compared to those in Pb-Pb collisions at $\sqrt{s_{NN}} = 5.02$ TeV with $z_{\text{cut}} = 0.2$ for 0%–10% centrality for $R = 0.2$ (left) and 30%–50% centrality for $R = 0.4$ (right). The distributions are normalized to the inclusive jet cross section in the $60 < p_{T,\text{ch jet}} < 80$ GeV/ c interval, and f_{tagged} indicates the fraction of splittings that were tagged to pass the SD condition in the selected $p_{T,\text{ch jet}}$ interval. The ratios in the bottom panel are compared to the following theoretical predictions: JETSCAPE [63], JEWEL [62,64], Caual *et al.* [34,65], Chien *et al.* [33], Qin *et al.* [35], and Pablos *et al.* [36,66,67]. Further details can be found in Ref. [50].

central collisions, the data suggests a narrowing of the Pb-Pb distribution relative to the pp distribution is observed. This narrowing persists even in semicentral Pb-Pb collisions for $R = 0.4$ where quenching effects are expected to be less than in central collisions.

We compare the ratio of the measurements in pp and Pb-Pb collisions with several theoretical implementations of jet quenching:

(i) JETSCAPE [63] consists of a medium-modified parton shower with the MATTER model [68] controlling

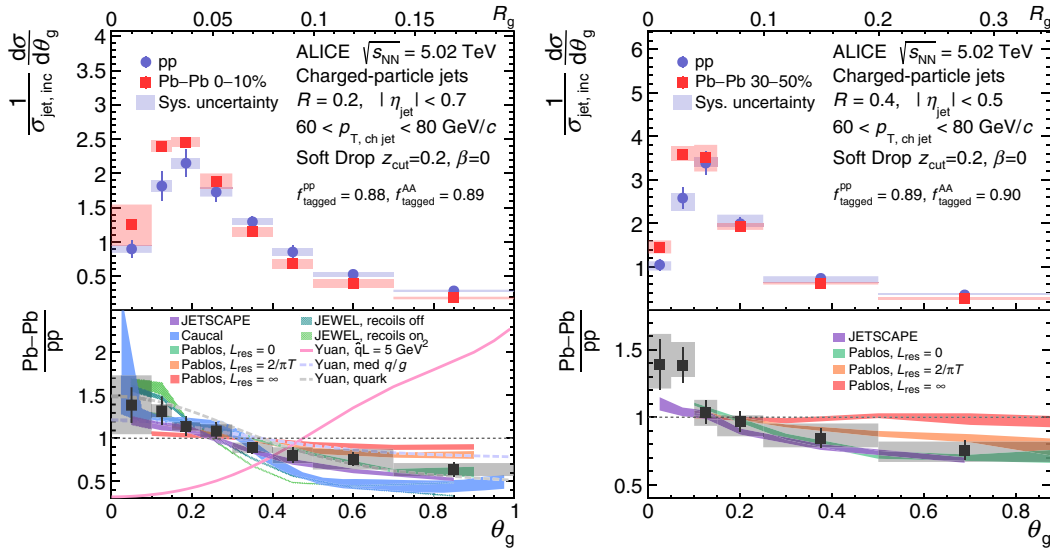


FIG. 3. Unfolded θ_g distributions for charged-particle jets in pp collisions compared to those in Pb-Pb collisions at $\sqrt{s_{NN}} = 5.02$ TeV with $z_{\text{cut}} = 0.2$ for 0%–10% centrality for $R = 0.2$ (left) and 30%–50% centrality for $R = 0.4$ (right). The distributions are normalized to the inclusive jet cross section in the $60 < p_{T,\text{ch jet}} < 80$ GeV/ c interval, and f_{tagged} indicates the fraction of splittings that were tagged to pass the SD condition in the selected $p_{T,\text{ch jet}}$ interval. The ratios in the bottom panel are compared to the following theoretical predictions: JETSCAPE [63], JEWEL [62,64], Caual *et al.* [34,65], Pablos *et al.* [36,66,67], and Yuan *et al.* [31]. Further details can be found in Ref. [50].

the high-virtuality phase and the Linear Boltzmann Transport (LBT) model describing the low-virtuality phase [69]. The version of JETSCAPE used for this calculation employs a jet transport coefficient, \hat{q} , that includes dependence on parton virtuality, in addition to dependence on the local temperature and running of the parton-medium coupling.

(ii) JEWEL [62,64] consists of a Monte Carlo implementation of Baier-Dokshitzer-Mueller-Peigne-Schiff-Zakharov-based medium-induced gluon radiation in a medium modeled with a Bjorken expansion. We consider the impact of medium recoil by including calculations both with and without recoils enabled [70].

(iii) Caucal *et al.* [34,65] implements a PQCD parton shower with incoherent interactions including both factorized vacuum and medium-induced emissions in a static brick medium.

(iv) Chien *et al.* [33] (for z_g only) applies Soft Collinear Effective Theory with Glauber gluon interactions.

(v) Qin *et al.* [35] (for z_g only) applies the higher twist formalism with coherent energy loss.

(vi) Pablos *et al.* [36,66,67] consists of partons produced by a vacuum shower that interact with the medium according to a strongly coupled AdS/CFT-based model. The parameter L_{res} describes the degree to which the medium can resolve the jet angular structure, where $L_{\text{res}} = 0$ corresponds to full resolution of all jet constituents (fully incoherent), $L_{\text{res}} = \infty$ corresponds to fully coherent energy loss, and $L_{\text{res}} = 2/\pi T$ is an intermediate case, where T is the local medium temperature.

(vii) Yuan *et al.* [31] (for θ_g only) “med q/g ” and “quark” consist of medium-modified quark-gluon fractions without any additional effects, where the quark-gluon fractions in the med q/g case are extracted in Ref. [71] with a relative suppression factor of approximately four between gluon jets and quark jets. The calculation labeled “ $\hat{q}L$ ” includes an implementation of transverse-momentum broadening.

The Pb-Pb-to- pp ratios of the z_g distributions are consistent with all theoretical predictions considered. The predicted modifications, which have been constrained by previous measurements [22,23], are small, and the differences between them are yet smaller than the current uncertainty of the data. Nevertheless, these new measurements are the first direct comparisons of predictions to fully corrected data, and limit the possible in-medium modifications of the momentum structure of hard splittings to be less than 10–20% depending on the centrality, jet R , and the grooming settings considered.

Despite employing different microscopic implementations of the jet-medium interactions, the majority of the models capture the qualitative feature of the narrowing seen in the θ_g distributions. The theoretical models can be grouped according to three distinct mechanisms by which θ_g is modified: incoherent energy loss, coherent energy

loss, and transverse broadening. The measurements are consistent with models implementing (transverse) incoherent interaction of the jet shower constituents with the medium. This is illustrated by calculations of Pablos *et al.* where the data favor the incoherent energy loss ($L_{\text{res}} = 0$) and is also supported by Caucal *et al.*, JEWEL, and JETSCAPE. On the other hand, the Yuan *et al.* calculation with medium-modified “quark-gluon” fractions indicates that the data could be explained by the stronger suppression of gluon showers, which are on average broader, with fully coherent energy loss. These two physics mechanisms—the degree of incoherent energy loss, and the relative quark-gluon suppression—both lead to a suppression of wide-angle splittings. The prediction by Yuan *et al.* $\hat{q}L$ exhibits the opposite trend compared to the data, demonstrating that there is no strong transverse broadening in the hard substructure.

The presented measurements indicate that the medium has a significant resolving power for splittings with a particular dependence on the angular (or coherence) scale, promoting narrow structures or filtering out wider jets altogether.

Conclusions.—We reported the groomed jet momentum fraction, z_g , and the (scaled) groomed jet radius, θ_g , of charged-particle jets measured in pp and Pb-Pb collisions at $\sqrt{s_{NN}} = 5.02$ TeV with the ALICE detector. By using stronger grooming conditions in the SD grooming algorithm, we suppressed contamination of mistagged splittings from the underlying event, and unfolded the final distributions for detector and background fluctuation effects. This allows for the first time the direct comparison of groomed jet measurements in heavy-ion collisions with theoretical predictions of jet quenching in the QGP. The z_g distributions are consistent with no modification in Pb-Pb collisions compared to pp collisions. The θ_g distributions are narrower in Pb-Pb collisions compared to pp collisions, which is the first direct experimental evidence for the modification of the angular scale of groomed jets in heavy-ion collisions.

These new results demonstrate sensitivity to the microscopic structure of the QGP, including its angular resolving power. This marks an important step towards quantitative understanding of the properties of the QGP, and provides a new path for novel differential jet substructure measurements to further elucidate the microscopic nature of the QGP.

We gratefully acknowledge Paul Caucal, Yang-Ting Chien, Daniel Pablos, Chanwook Park, Guang-You Qin, Gregory Soyez, Feng Yuan, and the JETSCAPE Collaboration for providing theoretical predictions. We thank Korinna Zapp for discussions regarding recoil subtraction in the JEWEL model. The ALICE Collaboration would like to thank all its engineers and technicians for their invaluable contributions to the construction of the experiment and the CERN accelerator teams for the

outstanding performance of the LHC complex. The ALICE Collaboration gratefully acknowledges the resources and support provided by all Grid centres and the Worldwide LHC Computing Grid (WLCG) Collaboration. The ALICE Collaboration acknowledges the following funding agencies for their support in building and running the ALICE detector: A. I. Alikhanyan National Science Laboratory (Yerevan Physics Institute) Foundation (ANSL), State Committee of Science and World Federation of Scientists (WFS), Armenia; Austrian Academy of Sciences, Austrian Science Fund (FWF): [M 2467-N36] and Nationalstiftung für Forschung, Technologie und Entwicklung, Austria; Ministry of Communications and High Technologies, National Nuclear Research Center, Azerbaijan; Conselho Nacional de Desenvolvimento Científico e Tecnológico (CNPq), Financiadora de Estudos e Projetos (Finep), Fundação de Amparo à Pesquisa do Estado de São Paulo (FAPESP) and Universidade Federal do Rio Grande do Sul (UFRGS), Brazil; Ministry of Education of China (MOEC), Ministry of Science & Technology of China (MSTC) and National Natural Science Foundation of China (NSFC), China; Ministry of Science and Education and Croatian Science Foundation, Croatia; Centro de Aplicaciones Tecnológicas y Desarrollo Nuclear (CEADEN), Cubaenergía, Cuba; Ministry of Education, Youth and Sports of the Czech Republic, Czech Republic; The Danish Council for Independent Research | Natural Sciences, the VILLUM FONDEN and Danish National Research Foundation (DNRF), Denmark; Helsinki Institute of Physics (HIP), Finland; Commissariat à l’Energie Atomique (CEA) and Institut National de Physique Nucléaire et de Physique des Particules (IN2P3) and Centre National de la Recherche Scientifique (CNRS), France; Bundesministerium für Bildung und Forschung (BMBF) and GSI Helmholtzzentrum für Schwerionenforschung GmbH, Germany; General Secretariat for Research and Technology, Ministry of Education, Research and Religions, Greece; National Research, Development and Innovation Office, Hungary; Department of Atomic Energy Government of India (DAE), Department of Science and Technology, Government of India (DST), University Grants Commission, Government of India (UGC) and Council of Scientific and Industrial Research (CSIR), India; Indonesian Institute of Science, Indonesia; Istituto Nazionale di Fisica Nucleare (INFN), Italy; Institute for Innovative Science and Technology, Nagasaki Institute of Applied Science (IIST), Japanese Ministry of Education, Culture, Sports, Science and Technology (MEXT) and Japan Society for the Promotion of Science (JSPS) KAKENHI, Japan; Consejo Nacional de Ciencia (CONACYT) y Tecnología, through Fondo de Cooperación Internacional en Ciencia y Tecnología (FONCICYT) and Dirección General de Asuntos del Personal Académico (DGAPA), Mexico; Nederlandse

Organisatie voor Wetenschappelijk Onderzoek (NWO), Netherlands; The Research Council of Norway, Norway; Commission on Science and Technology for Sustainable Development in the South (COMSATS), Pakistan; Pontificia Universidad Católica del Perú, Peru; Ministry of Education and Science, National Science Centre and WUT ID-UB, Poland; Korea Institute of Science and Technology Information and National Research Foundation of Korea (NRF), Republic of Korea; Ministry of Education and Scientific Research, Institute of Atomic Physics and Ministry of Research and Innovation and Institute of Atomic Physics, Romania; Joint Institute for Nuclear Research (JINR), Ministry of Education and Science of the Russian Federation, National Research Centre Kurchatov Institute, Russian Science Foundation and Russian Foundation for Basic Research, Russia; Ministry of Education, Science, Research and Sport of the Slovak Republic, Slovakia; National Research Foundation of South Africa, South Africa; Swedish Research Council (VR) and Knut & Alice Wallenberg Foundation (KAW), Sweden; European Organization for Nuclear Research, Switzerland; Suranaree University of Technology (SUT), National Science and Technology Development Agency (NSDTA) and Office of the Higher Education Commission under NRU project of Thailand, Thailand; Turkish Energy, Nuclear and Mineral Research Agency (TENMAK), Turkey; National Academy of Sciences of Ukraine, Ukraine; Science and Technology Facilities Council (STFC), United Kingdom; National Science Foundation of the United States of America (NSF) and United States Department of Energy, Office of Nuclear Physics (DOE NP), USA.

-
- [1] J. Adams *et al.* (STAR Collaboration), Experimental and theoretical challenges in the search for the quark gluon plasma: The STAR Collaboration’s critical assessment of the evidence from RHIC collisions, *Nucl. Phys.* **A757**, 102 (2005).
 - [2] K. Adcox *et al.* (PHENIX Collaboration), Formation of dense partonic matter in relativistic nucleus-nucleus collisions at RHIC: Experimental evaluation by the PHENIX collaboration, *Nucl. Phys.* **A757**, 184 (2005).
 - [3] B. Müller, J. Schukraft, and B. Wyslouch, First Results from Pb + Pb Collisions at the LHC, *Annu. Rev. Nucl. Part. Sci.* **62**, 361 (2012).
 - [4] P. Braun-Munzinger, V. Koch, T. Schäfer, and J. Stachel, Properties of hot and dense matter from relativistic heavy ion collisions, *Phys. Rep.* **621**, 76 (2016).
 - [5] W. Busza, K. Rajagopal, and W. van der Schee, Heavy Ion Collisions: The Big Picture, and the Big Questions, *Annu. Rev. Nucl. Part. Sci.* **68**, 339 (2018).
 - [6] J. D. Bjorken, Highly relativistic nucleus-nucleus collisions: The central rapidity region, *Phys. Rev. D* **27**, 140 (1983).

- [7] G.-Y. Qin and X.-N. Wang, Jet quenching in high-energy heavy-ion collisions, *Int. J. Mod. Phys. E* **24**, 1530014 (2015).
- [8] J.-P. Blaizot and Y. Mehtar-Tani, Jet structure in heavy ion collisions, *Int. J. Mod. Phys. E* **24**, 1530012 (2015).
- [9] A. Majumder and M. van Leeuwen, The theory and phenomenology of perturbative QCD based jet quenching, *Prog. Part. Nucl. Phys.* **66**, 41 (2011).
- [10] ALICE Collaboration, Measurements of inclusive jet spectra in pp and central Pb-Pb collisions at $\sqrt{s_{NN}} = 5.02$ TeV, *Phys. Rev. C* **101**, 034911 (2020).
- [11] ATLAS Collaboration, Measurement of the nuclear modification factor for inclusive jets in Pb + Pb collisions at $\sqrt{s_{NN}} = 5.02$ TeV with the ATLAS detector, *Phys. Lett. B* **790**, 108 (2019).
- [12] CMS Collaboration, Measurement of inclusive jet cross sections in pp and Pb-Pb collisions at $\sqrt{s_{NN}} = 2.76$ TeV, *Phys. Rev. C* **96**, 015202 (2017).
- [13] J. Adam *et al.* (STAR Collaboration), Measurement of inclusive charged-particle jet production in Au + Au collisions at $\sqrt{s_{NN}} = 200$ GeV, *Phys. Rev. C* **102**, 054913 (2020).
- [14] ALICE Collaboration, Measurement of jet quenching with semi-inclusive hadron-jet distributions in central Pb-Pb collisions at $\sqrt{s_{NN}} = 2.76$ TeV, *J. High Energy Phys.* **09** (2015) 170.
- [15] STAR Collaboration, Measurements of jet quenching with semi-inclusive hadron + jet distributions in Au + Au collisions at $\sqrt{s_{NN}} = 200$ GeV, *Phys. Rev. C* **96**, 024905 (2017).
- [16] ALICE Collaboration, Medium modification of the shape of small-radius jets in central Pb-Pb collisions at $\sqrt{s_{NN}} = 2.76$ TeV, *J. High Energy Phys.* **10** (2018) 139.
- [17] ATLAS Collaboration, Measurement of jet fragmentation in Pb-Pb and pp collisions at $\sqrt{s_{NN}} = 5.02$ TeV with the ATLAS detector, *Phys. Rev. C* **98**, 024908 (2018).
- [18] CMS Collaboration, Modification of jet shapes in Pb-Pb collisions at $\sqrt{s_{NN}} = 2.76$ TeV, *Phys. Lett. B* **730**, 243 (2014).
- [19] A. J. Larkoski, S. Marzani, G. Soyez, and J. Thaler, Soft Drop, *J. High Energy Phys.* **05** (2014) 146.
- [20] M. Dasgupta, A. Fregoso, S. Marzani, and G. P. Salam, Towards an understanding of jet substructure, *J. High Energy Phys.* **09** (2013) 029.
- [21] A. J. Larkoski, S. Marzani, and J. Thaler, Sudakov Safety in Perturbative QCD, *Phys. Rev. D* **91**, 111501 (2015).
- [22] CMS Collaboration, Measurement of the Splitting Function in pp and Pb-Pb Collisions at $\sqrt{s_{NN}} = 5.02$ TeV, *Phys. Rev. Lett.* **120**, 142302 (2018).
- [23] ALICE Collaboration, Exploration of jet substructure using iterative declustering in pp and Pb-Pb collisions at LHC energies, *Phys. Lett. B* **802**, 135227 (2020).
- [24] CMS Collaboration, Measurement of the groomed jet mass in Pb-Pb and pp collisions at $\sqrt{s_{NN}} = 5.02$ TeV, *J. High Energy Phys.* **10** (2018) 161.
- [25] Y. L. Dokshitzer, G. D. Leder, S. Moretti, and B. R. Webber, Better jet clustering algorithms, *J. High Energy Phys.* **08** (1997) 001.
- [26] ATLAS Collaboration, Measurement of soft-drop jet observables in pp collisions with the ATLAS detector at $\sqrt{s_{NN}} = 13$ TeV, *Phys. Rev. D* **101**, 052007 (2020).
- [27] CMS Collaboration, Measurement of jet substructure observables in $t\bar{t}$ events from proton-proton collisions at $\sqrt{s} = 13$ TeV, *Phys. Rev. D* **98**, 092014 (2018).
- [28] A. Tripathy, W. Xue, A. Larkoski, S. Marzani, and J. Thaler, Jet substructure studies with CMS open data, *Phys. Rev. D* **96**, 074003 (2017).
- [29] J. Adam *et al.* (STAR Collaboration), Measurement of groomed jet substructure observables in p + p collisions at $\sqrt{s} = 200$ GeV with STAR, *Phys. Lett. B* **811**, 135846 (2020).
- [30] Z.-B. Kang, K. Lee, X. Liu, D. Neill, and F. Ringer, The soft drop groomed jet radius at NLL, *J. High Energy Phys.* **02** (2020) 054.
- [31] F. Ringer, B.-W. Xiao, and F. Yuan, Can we observe jet P_T -broadening in heavy-ion collisions at the LHC?, *Phys. Lett. B* **808**, 135634 (2020).
- [32] J. Casalderrey-Solana, Y. Mehtar-Tani, C. A. Salgado, and K. Tywoniuk, New picture of jet quenching dictated by color coherence, *Phys. Lett. B* **725**, 357 (2013).
- [33] Y.-T. Chien and I. Vitev, Probing the Hardest Branching within Jets in Heavy-Ion Collisions, *Phys. Rev. Lett.* **119**, 112301 (2017).
- [34] P. Caucal, E. Iancu, and G. Soyez, Deciphering the z_g distribution in ultrarelativistic heavy ion collisions, *J. High Energy Phys.* **10** (2019) 273.
- [35] N.-B. Chang, S. Cao, and G.-Y. Qin, Probing medium-induced jet splitting and energy loss in heavy-ion collisions, *Phys. Lett. B* **781**, 423 (2018).
- [36] J. Casalderrey-Solana, G. Milhano, D. Pablos, and K. Rajagopal, Modification of Jet Substructure in Heavy Ion Collisions as a Probe of the Resolution Length of Quark-Gluon Plasma, *J. High Energy Phys.* **01** (2020) 044.
- [37] J. Mulligan and M. Ploskon, Identifying groomed jet splittings in heavy-ion collisions, *Phys. Rev. C* **102**, 044913 (2020).
- [38] K. Aamodt *et al.* (ALICE Collaboration), The ALICE experiment at the CERN LHC, *J. Instrum.* **3**, S08002 (2008).
- [39] ALICE Collaboration, Performance of the ALICE Experiment at the CERN LHC, *Int. J. Mod. Phys. A* **29**, 1430044 (2014).
- [40] ALICE Collaboration, Performance of the ALICE VZERO system, *J. Instrum.* **8**, P10016 (2013).
- [41] ALICE Collaboration, Centrality determination of Pb-Pb collisions at $\sqrt{s_{NN}} = 2.76$ TeV with ALICE, *Phys. Rev. C* **88**, 044909 (2013).
- [42] ALICE Collaboration, Centrality determination in heavy-ion collisions, <http://cds.cern.ch/record/2636623>.
- [43] ALICE Collaboration, ALICE 2017 luminosity determination for pp collisions at $\sqrt{s} = 5$ TeV, <http://cds.cern.ch/record/2648933>.
- [44] J. Alme *et al.*, The ALICE TPC, a large 3-dimensional tracking device with fast readout for ultra-high multiplicity events, *Nucl. Instrum. Methods Phys. Res., Sect. A* **622**, 316 (2010).
- [45] ALICE Collaboration, Alignment of the ALICE Inner Tracking System with cosmic-ray tracks, *J. Instrum.* **5**, P03003 (2010).
- [46] H.-M. Chang, M. Procura, J. Thaler, and W. J. Waalewijn, Calculating Track-Based Observables for the LHC, *Phys. Rev. Lett.* **111**, 102002 (2013).

- [47] H. Chen, I. Moult, X. Y. Zhang, and H. X. Zhu, Rethinking jets with energy correlators: Tracks, resummation, and analytic continuation, *Phys. Rev. D* **102**, 054012 (2020).
- [48] Y.-T. Chien, R. Rahn, S. Schrijnder van Velzen, D. Y. Shao, W. J. Waalewijn, and B. Wu, Recoil-free azimuthal angle for precision boson-jet correlation, *Phys. Lett. B* **815**, 136124 (2021).
- [49] G. Aad *et al.* (ATLAS Collaboration), Measurement of soft-drop jet observables in pp collisions with the ATLAS detector at $\sqrt{s} = 13$ TeV, *Phys. Rev. D* **101**, 052007 (2020).
- [50] ALICE Collaboration, Supplemental material: Measurements of the groomed jet radius and groomed momentum fraction in pp and Pb–Pb collisions at $\sqrt{s_{NN}} = 5.02$ TeV, <https://cds.cern.ch/record/2725572>.
- [51] M. Cacciari, G. P. Salam, and G. Soyez, FastJet User Manual, *Eur. Phys. J. C* **72**, 1896 (2012).
- [52] M. Cacciari, G. P. Salam, and G. Soyez, The anti- k_r jet clustering algorithm, *J. High Energy Phys.* **04** (2008) 063.
- [53] M. Cacciari, G. P. Salam, and G. Soyez, The Catchment Area of Jets, *J. High Energy Phys.* **04** (2008) 005.
- [54] ALICE Collaboration, Measurement of event background fluctuations for charged particle jet reconstruction in Pb–Pb collisions at $\sqrt{s_{NN}} = 2.76$ TeV, *J. High Energy Phys.* **03** (2012) 053.
- [55] P. Berta, M. Spousta, D. W. Miller, and R. Leitner, Particle-level pileup subtraction for jets and jet shapes, *J. High Energy Phys.* **06** (2014) 092.
- [56] P. Berta, L. Masetti, D. Miller, and M. Spousta, Pileup and Underlying Event Mitigation with Iterative Constituent Subtraction, *J. High Energy Phys.* **08** (2019) 175.
- [57] T. Sjostrand, S. Ask, J. R. Christiansen, R. Corke, N. Desai, P. Ilten, S. Mrenna, S. Prestel, C. O. Rasmussen, and P. Z. Skands, An introduction to PYTHIA8.2, *Comput. Phys. Commun.* **191**, 159 (2015).
- [58] R. Brun, F. Bruyant, M. Maire, A. C. McPherson, and P. Zanmarini, GEANT3: User's guide GEANT3.10, GEANT3.11; rev. version, CERN, Geneva, 1987.
- [59] G. D'Agostini, A multidimensional unfolding method based on bayes' theorem, *Nucl. Instrum. Methods Phys. Res., Sect. A* **362**, 487 (1995).
- [60] RooUnfold, <http://hepunix.rl.ac.uk/~adye/software/unfold/RooUnfold.html> (Access date: May 31 2020).
- [61] J. Bellm *et al.*, HERWIG7.0/HERWIG++ 3.0 release note, *Eur. Phys. J. C* **76**, 196 (2016).
- [62] K. C. Zapp, JEWEL 2.0.0: Directions for use, *Eur. Phys. J. C* **74**, 2762 (2014).
- [63] J. Putschke *et al.* (JETSCAPE Collaboration), The JETSCAPE framework, [arXiv:1903.07706](https://arxiv.org/abs/1903.07706).
- [64] K. C. Zapp, F. Krauss, and U. A. Wiedemann, A perturbative framework for jet quenching, *J. High Energy Phys.* **03** (2013) 080.
- [65] P. Caucal, E. Iancu, A. H. Mueller, and G. Soyez, Vacuum-Like Jet Fragmentation in a Dense QCD Medium, *Phys. Rev. Lett.* **120**, 232001 (2018).
- [66] J. Casalderrey-Solana, D. C. Gulhan, J. G. Milhano, D. Pablos, and K. Rajagopal, A Hybrid Strong/Weak Coupling Approach to Jet Quenching, *J. High Energy Phys.* **10** (2014) 019; **09** (2015) 175(E).
- [67] Z. Hulcher, D. Pablos, and K. Rajagopal, Resolution effects in the Hybrid strong/weak coupling model, *J. High Energy Phys.* **03** (2018) 010.
- [68] A. Majumder, Incorporating space-time within medium-modified jet event generators, *Phys. Rev. C* **88**, 014909 (2013).
- [69] Y. He, T. Luo, X.-N. Wang, and Y. Zhu, Linear Boltzmann transport for jet propagation in the quark-gluon plasma: Elastic processes and medium recoil, *Phys. Rev. C* **91**, 054908 (2015); **97**, 019902(E) (2018).
- [70] R. Kunnawalkam Elayavalli and K. C. Zapp, Medium response in JEWEL and its impact on jet shape observables in heavy ion collisions, *J. High Energy Phys.* **07** (2017) 141.
- [71] J.-W. Qiu, F. Ringer, N. Sato, and P. Zurita, Factorization of Jet Cross Sections in Heavy-Ion Collisions, *Phys. Rev. Lett.* **122**, 252301 (2019).

S. Acharya,¹⁴³ D. Adamová,⁹⁸ A. Adler,⁷⁶ G. Aglieri Rinella,³⁵ M. Agnello,³¹ N. Agrawal,⁵⁵ Z. Ahammed,¹⁴³ S. Ahmad,¹⁶ S. U. Ahn,⁷⁸ I. Ahuja,³⁹ Z. Akbar,⁵² A. Akindinov,⁹⁵ M. Al-Turany,¹¹⁰ S. N. Alam,^{16,41} D. Aleksandrov,⁹¹ B. Alessandro,⁶¹ H. M. Alfanda,⁷ R. Alfaro Molina,⁷³ B. Ali,¹⁶ Y. Ali,¹⁴ A. Alici,²⁶ N. Alizadehvandchali,¹²⁷ A. Alkin,³⁵ J. Alme,²¹ T. Alt,⁷⁰ L. Altenkamper,²¹ I. Altsybeev,¹¹⁵ M. N. Anaam,⁷ C. Andrei,⁴⁹ D. Andreou,⁹³ A. Andronic,¹⁴⁶ M. Angeletti,³⁵ V. Anguelov,¹⁰⁷ F. Antinori,⁵⁸ P. Antonioli,⁵⁵ C. Anuj,¹⁶ N. Apadula,⁸² L. Aphecetche,¹¹⁷ H. Appelshäuser,⁷⁰ S. Arcelli,²⁶ R. Arnaldi,⁶¹ I. C. Arsene,²⁰ M. Arslanodok,^{107,148} A. Augustinus,³⁵ R. Averbeck,¹¹⁰ S. Aziz,⁸⁰ M. D. Azmi,¹⁶ A. Badalà,⁵⁷ Y. W. Baek,⁴² X. Bai,^{110,131} R. Bailhache,⁷⁰ Y. Bailung,⁵¹ R. Bala,¹⁰⁴ A. Balbino,³¹ A. Baldisseri,¹⁴⁰ B. Balis,² M. Ball,⁴⁴ D. Banerjee,⁴ R. Barbera,²⁷ L. Barioglio,¹⁰⁸ M. Barlou,⁸⁷ G. G. Barnaföldi,¹⁴⁷ L. S. Barnby,⁹⁷ V. Barret,¹³⁷ C. Bartels,¹³⁰ K. Barth,³⁵ E. Bartsch,⁷⁰ F. Baruffaldi,²⁸ N. Bastid,¹³⁷ S. Basu,⁸³ G. Batigne,¹¹⁷ B. Batyunya,⁷⁷ D. Bauri,⁵⁰ J. L. Bazo Alba,¹¹⁴ I. G. Bearden,⁹² C. Beattie,¹⁴⁸ I. Belikov,¹³⁹ A. D. C. Bell Hechavarria,¹⁴⁶ F. Bellini,²⁶ R. Bellwied,¹²⁷ S. Belokurova,¹¹⁵ V. Belyaev,⁹⁶ G. Bencedi,⁷¹ S. Beole,²⁵ A. Bercuci,⁴⁹ Y. Berdnikov,¹⁰¹ A. Berdnikova,¹⁰⁷ L. Bergmann,¹⁰⁷ M. G. Besoiu,⁶⁹ L. Betev,³⁵ P. P. Bhaduri,¹⁴³ A. Bhasin,¹⁰⁴ I. R. Bhat,¹⁰⁴ M. A. Bhat,⁴ B. Bhattacharjee,⁴³ P. Bhattacharya,²³ L. Bianchi,²⁵ N. Bianchi,⁵³ J. Bielčák,³⁸ J. Bielčiková,⁹⁸ J. Biernat,¹²⁰ A. Bilandzic,¹⁰⁸ G. Biro,¹⁴⁷ S. Biswas,⁴ J. T. Blair,¹²¹ D. Blau,^{84,91} M. B. Blidaru,¹¹⁰ C. Blume,⁷⁰ G. Boca,^{29,59} F. Bock,⁹⁹ A. Bogdanov,⁹⁶ S. Boi,²³ J. Bok,⁶³ L. Boldizsár,¹⁴⁷ A. Bolozdynya,⁹⁶ M. Bombara,³⁹ P. M. Bond,³⁵ G. Bonomi,^{59,142} H. Borel,¹⁴⁰ A. Borissova,⁸⁴ H. Bossi,¹⁴⁸ E. Botta,²⁵

L. Bratrud,⁷⁰ P. Braun-Munzinger,¹¹⁰ M. Bregant,¹²³ M. Broz,³⁸ G. E. Bruno,^{34,109} M. D. Buckland,¹³⁰ D. Budnikov,¹¹¹ H. Buesching,⁷⁰ S. Bufalino,³¹ O. Bugnon,¹¹⁷ P. Buhler,¹¹⁶ Z. Buthelezi,^{74,134} J. B. Butt,¹⁴ S. A. Bysiak,¹²⁰ M. Cai,^{7,28} H. Caines,¹⁴⁸ A. Caliva,¹¹⁰ E. Calvo Villar,¹¹⁴ J. M. M. Camacho,¹²² R. S. Camacho,⁴⁶ P. Camerini,²⁴ F. D. M. Canedo,¹²³ F. Carnesecchi,^{26,35} R. Caron,¹⁴⁰ J. Castillo Castellanos,¹⁴⁰ E. A. R. Casula,²³ F. Catalano,³¹ C. Ceballos Sanchez,⁷⁷ P. Chakraborty,⁵⁰ S. Chandra,¹⁴³ S. Chapeland,³⁵ M. Chartier,¹³⁰ S. Chattopadhyay,¹⁴³ S. Chattopadhyay,¹¹² A. Chauvin,²³ T. G. Chavez,⁴⁶ T. Cheng,⁷ C. Cheshkov,¹³⁸ B. Cheynis,¹³⁸ V. Chibante Barroso,³⁵ D. D. Chinellato,¹²⁴ S. Cho,⁶³ P. Chochula,³⁵ P. Christakoglou,⁹³ C. H. Christensen,⁹² P. Christiansen,⁸³ T. Chujo,¹³⁶ C. Cicalo,⁵⁶ L. Cifarelli,²⁶ F. Cindolo,⁵⁵ M. R. Ciupek,¹¹⁰ G. Clai,^{55,b} J. Cleymans,^{126,a} F. Colamaria,⁵⁴ J. S. Colburn,¹¹³ D. Colella,^{34,54,109,147} A. Collu,⁸² M. Colocci,³⁵ M. Concas,^{61,c} G. Conesa Balbastre,⁸¹ Z. Conesa del Valle,⁸⁰ G. Contin,²⁴ J. G. Contreras,³⁸ M. L. Coquet,¹⁴⁰ T. M. Cormier,⁹⁹ P. Cortese,³² M. R. Cosentino,¹²⁵ F. Costa,³⁵ S. Costanza,^{29,59} P. Crochet,¹³⁷ R. Cruz-Torres,⁸² E. Cuautle,⁷¹ P. Cui,⁷ L. Cunqueiro,⁹⁹ A. Dainese,⁵⁸ M. C. Danisch,¹⁰⁷ A. Danu,⁶⁹ I. Das,¹¹² P. Das,⁸⁹ P. Das,⁴ S. Das,⁴ S. Dash,⁵⁰ S. De,⁸⁹ A. De Caro,³⁰ G. de Cataldo,⁵⁴ L. De Cilladi,²⁵ J. de Cuveland,⁴⁰ A. De Falco,²³ D. De Gruttola,³⁰ N. De Marco,⁶¹ C. De Martin,²⁴ S. De Pasquale,³⁰ S. Deb,⁵¹ H. F. Degenhardt,¹²³ K. R. Deja,¹⁴⁴ L. Dello Stritto,³⁰ S. Delsanto,²⁵ W. Deng,⁷ P. Dhankher,¹⁹ D. Di Bari,³⁴ A. Di Mauro,³⁵ R. A. Diaz,⁸ T. Dietel,¹²⁶ Y. Ding,^{7,138} R. Divià,³⁵ D. U. Dixit,¹⁹ Ø. Djuvsland,²¹ U. Dmitrieva,⁶⁵ J. Do,⁶³ A. Dobrin,⁶⁹ B. Dönigus,⁷⁰ O. Dordic,²⁰ A. K. Dubey,¹⁴³ A. Dubla,^{93,110} S. Dudi,¹⁰³ M. Dukhishyam,⁸⁹ P. Dupieux,¹³⁷ N. Dzalaiova,¹³ T. M. Eder,¹⁴⁶ R. J. Ehlers,⁹⁹ V. N. Eikeland,²¹ F. Eisenhut,⁷⁰ D. Elia,⁵⁴ B. Erazmus,¹¹⁷ F. Ercolessi,²⁶ F. Erhardt,¹⁰² A. Erokhin,¹¹⁵ M. R. Ersdal,²¹ B. Espagnon,⁸⁰ G. Eulisse,³⁵ D. Evans,¹¹³ S. Evdokimov,⁹⁴ L. Fabbietti,¹⁰⁸ M. Faggin,²⁸ J. Faivre,⁸¹ F. Fan,⁷ A. Fantoni,⁵³ M. Fasel,⁹⁹ P. Fecchio,³¹ A. Feliciello,⁶¹ G. Feofilov,¹¹⁵ A. Fernández Téllez,⁴⁶ A. Ferrero,¹⁴⁰ A. Ferretti,²⁵ V. J. G. Feuillard,¹⁰⁷ J. Figiel,¹²⁰ S. Filchagin,¹¹¹ D. Finogeev,⁶⁵ F. M. Fionda,^{21,56} G. Fiorenza,^{35,109} F. Flor,¹²⁷ A. N. Flores,¹²¹ S. Foertsch,⁷⁴ P. Foka,¹¹⁰ S. Fokin,⁹¹ E. Fragiaco,⁶² E. Frajna,¹⁴⁷ U. Fuchs,³⁵ N. Funicello,³⁰ C. Furget,⁸¹ A. Furs,⁶⁵ J. J. Gaardhøje,⁹² M. Gagliardi,²⁵ A. M. Gago,¹¹⁴ A. Gal,¹³⁹ C. D. Galvan,¹²² P. Ganoti,⁸⁷ C. Garabatos,¹¹⁰ J. R. A. Garcia,⁴⁶ E. Garcia-Solis,¹⁰ K. Garg,¹¹⁷ C. Gargiulo,³⁵ A. Garibli,⁹⁰ K. Garner,¹⁴⁶ P. Gasik,¹¹⁰ E. F. Gauger,¹²¹ A. Gautam,¹²⁹ M. B. Gay Ducati,⁷² M. Germain,¹¹⁷ P. Ghosh,¹⁴³ S. K. Ghosh,⁴ M. Giacalone,²⁶ P. Gianotti,⁵³ P. Giubellino,^{61,110} P. Giubilato,²⁸ A. M. C. Glaenger,¹⁴⁰ P. Glässel,¹⁰⁷ D. J. Q. Goh,⁸⁵ V. Gonzalez,¹⁴⁵ L. H. González-Trueba,⁷³ S. Gorbunov,⁴⁰ M. Gorgon,² L. Görlich,¹²⁰ S. Gotovac,³⁶ V. Grabski,⁷³ L. K. Graczykowski,¹⁴⁴ L. Greiner,⁸² A. Grelli,⁶⁴ C. Grigoras,³⁵ V. Grigoriev,⁹⁶ S. Grigoryan,^{1,77} O. S. Groetvik,²¹ F. Grosa,^{35,61} J. F. Grosse-Oetringhaus,³⁵ R. Grosso,¹¹⁰ G. G. Guardiano,¹²⁴ R. Guernane,⁸¹ M. Guilbaud,¹¹⁷ K. Gulbrandsen,⁹² T. Gunji,¹³⁵ W. Guo,⁷ A. Gupta,¹⁰⁴ R. Gupta,¹⁰⁴ S. P. Guzman,⁴⁶ L. Gyulai,¹⁴⁷ M. K. Habib,¹¹⁰ C. Hadjidakis,⁸⁰ G. Halimoglu,⁷⁰ H. Hamagaki,⁸⁵ G. Hamar,¹⁴⁷ M. Hamid,⁷ R. Hannigan,¹²¹ M. R. Haque,^{89,144} A. Harlenderova,¹¹⁰ J. W. Harris,¹⁴⁸ A. Harton,¹⁰ J. A. Hasenbichler,³⁵ H. Hassan,⁹⁹ D. Hatzifotiadou,⁵⁵ P. Hauer,⁴⁴ L. B. Havener,¹⁴⁸ S. Hayashi,¹³⁵ S. T. Heckel,¹⁰⁸ E. Hellbär,¹¹⁰ H. Helstrup,³⁷ T. Herman,³⁸ E. G. Hernandez,⁴⁶ G. Herrera Corral,⁹ F. Herrmann,¹⁴⁶ K. F. Hetland,³⁷ H. Hillemanns,³⁵ C. Hills,¹³⁰ B. Hippolyte,¹³⁹ B. Hofman,⁶⁴ B. Hohlweger,⁹³ J. Honermann,¹⁴⁶ G. H. Hong,¹⁴⁹ D. Horak,³⁸ S. Hornung,¹¹⁰ A. Horzyk,² R. Hosokawa,¹⁵ Y. Hou,⁷ P. Hristov,³⁵ C. Hughes,¹³³ P. Huhn,⁷⁰ T. J. Humanic,¹⁰⁰ H. Hushnud,¹¹² L. A. Husova,¹⁴⁶ A. Hutson,¹²⁷ D. Hutter,⁴⁰ J. P. Iddon,^{35,130} R. Ilkaev,¹¹¹ H. Ilyas,¹⁴ M. Inaba,¹³⁶ G. M. Innocenti,³⁵ M. Ippolitov,⁹¹ A. Isakov,^{38,98} M. S. Islam,¹¹² M. Ivanov,¹¹⁰ V. Ivanov,¹⁰¹ V. Izucheev,⁹⁴ M. Jablonski,² B. Jacak,⁸² N. Jacazio,³⁵ P. M. Jacobs,⁸² S. Jadlovská,¹¹⁹ J. Jadlovsky,¹¹⁹ S. Jaelani,⁶⁴ C. Jahnke,^{123,124} M. J. Jakubowska,¹⁴⁴ A. Jalotra,¹⁰⁴ M. A. Janik,¹⁴⁴ T. Janson,⁷⁶ M. Jercic,¹⁰² O. Jevons,¹¹³ A. A. P. Jimenez,⁷¹ F. Jonas,^{99,146} P. G. Jones,¹¹³ J. M. Jowett,^{35,110} J. Jung,⁷⁰ M. Jung,⁷⁰ A. Junique,³⁵ A. Jusko,¹¹³ J. Kaewjai,¹¹⁸ P. Kalinak,⁶⁶ A. Kalweit,³⁵ V. Kaplin,⁹⁶ S. Kar,⁷ A. Karasu Uysal,⁷⁹ D. Karatovic,¹⁰² O. Karavichev,⁶⁵ T. Karavicheva,⁶⁵ P. Karczmarczyk,¹⁴⁴ E. Karpechev,⁶⁵ A. Kazantsev,⁹¹ U. Keschull,⁷⁶ R. Keidel,⁴⁸ D. L. D. Keijdener,⁶⁴ M. Keil,³⁵ B. Ketzer,⁴⁴ Z. Khabanova,⁹³ A. M. Khan,⁷ S. Khan,¹⁶ A. Khanzadeev,¹⁰¹ Y. Kharlov,^{84,94} A. Khatun,¹⁶ A. Khuntia,¹²⁰ B. Kileng,³⁷ B. Kim,^{17,63} C. Kim,¹⁷ D. J. Kim,¹²⁸ E. J. Kim,⁷⁵ J. Kim,¹⁴⁹ J. S. Kim,⁴² J. Kim,¹⁰⁷ J. Kim,¹⁴⁹ J. Kim,⁷⁵ M. Kim,¹⁰⁷ S. Kim,¹⁸ T. Kim,¹⁴⁹ S. Kirsch,⁷⁰ I. Kisel,⁴⁰ S. Kiselev,⁹⁵ A. Kisiel,¹⁴⁴ J. P. Kitowski,² J. L. Klay,⁶ J. Klein,³⁵ S. Klein,⁸² C. Klein-Bösing,¹⁴⁶ M. Kleiner,⁷⁰ T. Klemenz,¹⁰⁸ A. Kluge,³⁵ A. G. Knospe,¹²⁷ C. Kobdaj,¹¹⁸ M. K. Köhler,¹⁰⁷ T. Kollegger,¹¹⁰ A. Kondratyev,⁷⁷ N. Kondratyeva,⁹⁶ E. Kondratyuk,⁹⁴ J. König,⁷⁰ S. A. Königstorfer,¹⁰⁸ P. J. Konopka,^{2,35} G. Kornakov,¹⁴⁴ S. D. Koryciak,² L. Koska,¹¹⁹ A. Kotliarov,⁹⁸ O. Kovalenko,⁸⁸ V. Kovalenko,¹¹⁵ M. Kowalski,¹²⁰ I. Králik,⁶⁶ A. Kravčáková,³⁹ L. Kreis,¹¹⁰ M. Krivda,^{66,113} F. Krizek,⁹⁸ K. Krizkova Gajdosova,³⁸ M. Kroesen,¹⁰⁷ M. Krüger,⁷⁰ E. Kryshen,¹⁰¹ M. Krzewicki,⁴⁰ V. Kučera,³⁵ C. Kuhn,¹³⁹ P. G. Kuijer,⁹³ T. Kumaoka,¹³⁶

D. Kumar,¹⁴³ L. Kumar,¹⁰³ N. Kumar,¹⁰³ S. Kundu,^{35,89} P. Kurashvili,⁸⁸ A. Kurepin,⁶⁵ A. B. Kurepin,⁶⁵ A. Kuryakin,¹¹¹ S. Kushpil,⁹⁸ J. Kvapil,¹¹³ M. J. Kweon,⁶³ J. Y. Kwon,⁶³ Y. Kwon,¹⁴⁹ S. L. La Pointe,⁴⁰ P. La Rocca,²⁷ Y. S. Lai,⁸² A. Lakrathok,¹¹⁸ M. Lamanna,³⁵ R. Langoy,¹³² K. Lapidus,³⁵ P. Larionov,^{35,53} E. Laudi,³⁵ L. Lautner,^{35,108} R. Lavicka,³⁸ T. Lazareva,¹¹⁵ R. Lea,^{24,59,142} J. Lehrbach,⁴⁰ R. C. Lemmon,⁹⁷ I. León Monzón,¹²² E. D. Lesser,¹⁹ M. Lettrich,^{35,108} P. Lévai,¹⁴⁷ X. Li,¹¹ X. L. Li,⁷ J. Lien,¹³² R. Lietava,¹¹³ B. Lim,¹⁷ S. H. Lim,¹⁷ V. Lindenstruth,⁴⁰ A. Lindner,⁴⁹ C. Lippmann,¹¹⁰ A. Liu,¹⁹ D. H. Liu,⁷ J. Liu,¹³⁰ I. M. Lofnes,²¹ V. Loginov,⁹⁶ C. Loizides,⁹⁹ P. Loncar,³⁶ J. A. Lopez,¹⁰⁷ X. Lopez,¹³⁷ E. López Torres,⁸ J. R. Luhder,¹⁴⁶ M. Lunardon,²⁸ G. Luparello,⁶² Y. G. Ma,⁴¹ A. Maevskaya,⁶⁵ M. Mager,³⁵ T. Mahmoud,⁴⁴ A. Maire,¹³⁹ M. Malaev,¹⁰¹ N. M. Malik,¹⁰⁴ Q. W. Malik,²⁰ L. Malinina,^{77,d} D. Mal'Kevich,⁹⁵ N. Mallick,⁵¹ P. Malzacher,¹¹⁰ G. Mandaglio,^{33,57} V. Manko,⁹¹ F. Manso,¹³⁷ V. Manzari,⁵⁴ Y. Mao,⁷ J. Mareš,⁶⁸ G. V. Margagliotti,²⁴ A. Margotti,⁵⁵ A. Marín,¹¹⁰ C. Markert,¹²¹ M. Marquard,⁷⁰ N. A. Martin,¹⁰⁷ P. Martinengo,³⁵ J. L. Martinez,¹²⁷ M. I. Martínez,⁴⁶ G. Martínez García,¹¹⁷ S. Masciocchi,¹¹⁰ M. Maserà,²⁵ A. Masoni,⁵⁶ L. Massacrier,⁸⁰ A. Mastroserio,^{54,141} A. M. Mathis,¹⁰⁸ O. Matonoha,⁸³ P. F. T. Matuoka,¹²³ A. Matyja,¹²⁰ C. Mayer,¹²⁰ A. L. Mazuecos,³⁵ F. Mazzaschi,²⁵ M. Mazzilli,³⁵ M. A. Mazzoni,^{60,a} J. E. Mdhluli,¹³⁴ A. F. Mechler,⁷⁰ F. Meddi,²² Y. Melikyan,⁶⁵ A. Menchaca-Rocha,⁷³ E. Meninno,^{30,116} A. S. Menon,¹²⁷ M. Meres,¹³ S. Mhlanga,^{74,126} Y. Miake,¹³⁶ L. Micheletti,^{25,61} L. C. Migliorin,¹³⁸ D. L. Mihaylov,¹⁰⁸ K. Mikhaylov,^{77,95} A. N. Mishra,¹⁴⁷ D. Miśkowiec,¹¹⁰ A. Modak,⁴ A. P. Mohanty,⁶⁴ B. Mohanty,⁸⁹ M. Mohisin Khan,^{16,e} M. A. Molander,⁴⁵ Z. Moravcova,⁹² C. Mordasini,¹⁰⁸ D. A. Moreira De Godoy,¹⁴⁶ L. A. P. Moreno,⁴⁶ I. Morozov,⁶⁵ A. Morsch,³⁵ T. Mrnjavac,³⁵ V. Muccifora,⁵³ E. Mudnic,³⁶ D. Mühlheim,¹⁴⁶ S. Muhuri,¹⁴³ J. D. Mulligan,⁸² A. Mulliri,²³ M. G. Munhoz,¹²³ R. H. Munzer,⁷⁰ H. Murakami,¹³⁵ S. Murray,¹²⁶ L. Musa,³⁵ J. Musinsky,⁶⁶ J. W. Myrcha,¹⁴⁴ B. Naik,^{50,134} R. Nair,⁸⁸ B. K. Nandi,⁵⁰ R. Nania,⁵⁵ E. Nappi,⁵⁴ A. F. Nassirpour,⁸³ A. Nath,¹⁰⁷ C. Natrass,¹³³ A. Neagu,²⁰ L. Nellen,⁷¹ S. V. Nesbo,³⁷ G. Neskovic,⁴⁰ D. Nesterov,¹¹⁵ B. S. Nielsen,⁹² S. Nikolaev,⁹¹ S. Nikulin,⁹¹ V. Nikulin,¹⁰¹ F. Noferini,⁵⁵ S. Noh,¹² P. Nomokonov,⁷⁷ J. Norman,¹³⁰ N. Novitzky,¹³⁶ P. Nowakowski,¹⁴⁴ A. Nyanin,⁹¹ J. Nystrand,²¹ M. Ogino,⁸⁵ A. Ohlson,⁸³ V. A. Okorokov,⁹⁶ J. Oleniacz,¹⁴⁴ A. C. Oliveira Da Silva,¹³³ M. H. Oliver,¹⁴⁸ A. Onnerstad,¹²⁸ C. Oppedisano,⁶¹ A. Ortiz Velasquez,⁷¹ T. Osako,⁴⁷ A. Oskarsson,⁸³ J. Otwinowski,¹²⁰ M. Oya,⁴⁷ K. Oyama,⁸⁵ Y. Pachmayer,¹⁰⁷ S. Padhan,⁵⁰ D. Pagano,^{59,142} G. Paic,⁷¹ A. Palasciano,⁵⁴ J. Pan,¹⁴⁵ S. Panebianco,¹⁴⁰ P. Pareek,¹⁴³ J. Park,⁶³ J. E. Parkkila,¹²⁸ S. P. Pathak,¹²⁷ R. N. Patra,^{35,104} B. Paul,²³ H. Pei,⁷ T. Peitzmann,⁶⁴ X. Peng,⁷ L. G. Pereira,⁷² H. Pereira Da Costa,¹⁴⁰ D. Peresunko,^{84,91} G. M. Perez,⁸ S. Perrin,¹⁴⁰ Y. Pestov,⁵ V. Petráček,³⁸ M. Petrovici,⁴⁹ R. P. Pezzi,^{72,117} S. Piano,⁶² M. Pikna,¹³ P. Pillot,¹¹⁷ O. Pinazza,^{35,55} L. Pinsky,¹²⁷ C. Pinto,²⁷ S. Pisano,⁵³ M. Płoskoń,⁸² M. Planinic,¹⁰² F. Pliquet,⁷⁰ M. G. Poghosyan,⁹⁹ B. Polichtchouk,⁹⁴ S. Politano,³¹ N. Poljak,¹⁰² A. Pop,⁴⁹ S. Porteboeuf-Houssais,¹³⁷ J. Porter,⁸² V. Pozdniakov,⁷⁷ S. K. Prasad,⁴ R. Preghenella,⁵⁵ F. Prino,⁶¹ C. A. Pruneau,¹⁴⁵ I. Pshenichnov,⁶⁵ M. Puccio,³⁵ S. Qiu,⁹³ L. Quaglia,²⁵ R. E. Quishpe,¹²⁷ S. Ragoni,¹¹³ A. Rakotozafindrabe,¹⁴⁰ L. Ramello,³² F. Rami,¹³⁹ S. A. R. Ramirez,⁴⁶ A. G. T. Ramos,³⁴ T. A. Rancien,⁸¹ R. Raniwala,¹⁰⁵ S. Raniwala,¹⁰⁵ S. S. Räsänen,⁴⁵ R. Rath,⁵¹ I. Ravasenga,⁹³ K. F. Read,^{99,133} A. R. Redelbach,⁴⁰ K. Redlich,^{88,f} A. Rehman,²¹ P. Reichelt,⁷⁰ F. Reidt,³⁵ H. A. Reme-ness,³⁷ R. Renfordt,⁷⁰ Z. Rescakova,³⁹ K. Reygers,¹⁰⁷ A. Riabov,¹⁰¹ V. Riabov,¹⁰¹ T. Richert,⁸³ M. Richter,²⁰ W. Riegler,³⁵ F. Riggi,²⁷ C. Ristea,⁶⁹ M. Rodríguez Cahuanti,⁴⁶ K. Røed,²⁰ R. Rogalev,⁹⁴ E. Rogochaya,⁷⁷ T. S. Rogoschinski,⁷⁰ D. Rohr,³⁵ D. Röhrich,²¹ P. F. Rojas,⁴⁶ P. S. Rokita,¹⁴⁴ F. Ronchetti,⁵³ A. Rosano,^{33,57} E. D. Rosas,⁷¹ A. Rossi,⁵⁸ A. Rotondi,^{29,59} A. Roy,⁵¹ P. Roy,¹¹² S. Roy,⁵⁰ N. Rubini,²⁶ O. V. Rueda,⁸³ R. Rui,²⁴ B. Rumyantsev,⁷⁷ P. G. Russek,² A. Rustamov,⁹⁰ E. Ryabinkin,⁹¹ Y. Ryabov,¹⁰¹ A. Rybicki,¹²⁰ H. Rytkonen,¹²⁸ W. Rzesza,¹⁴⁴ O. A. M. Saarimaki,⁴⁵ R. Sadek,¹¹⁷ S. Sadovskiy,⁹⁴ J. Saetre,²¹ K. Šafařík,³⁸ S. K. Saha,¹⁴³ S. Saha,⁸⁹ B. Sahoo,⁵⁰ P. Sahoo,⁵⁰ R. Sahoo,⁵¹ S. Sahoo,⁶⁷ D. Sahu,⁵¹ P. K. Sahu,⁶⁷ J. Saini,¹⁴³ S. Sakai,¹³⁶ S. Sambyal,¹⁰⁴ V. Samsonov,^{96,101,a} D. Sarkar,¹⁴⁵ N. Sarkar,¹⁴³ P. Sarma,⁴³ V. M. Sarti,¹⁰⁸ M. H. P. Sas,¹⁴⁸ J. Schambach,^{99,121} H. S. Scheid,⁷⁰ C. Schiaua,⁴⁹ R. Schicker,¹⁰⁷ A. Schmah,¹⁰⁷ C. Schmidt,¹¹⁰ H. R. Schmidt,¹⁰⁶ M. O. Schmidt,³⁵ M. Schmidt,¹⁰⁶ N. V. Schmidt,^{70,99} A. R. Schmier,¹³³ R. Schotter,¹³⁹ J. Schukraft,³⁵ Y. Schutz,¹³⁹ K. Schwarz,¹¹⁰ K. Schweda,¹¹⁰ G. Scioli,²⁶ E. Scomparin,⁶¹ J. E. Seger,¹⁵ Y. Sekiguchi,¹³⁵ D. Sekihata,¹³⁵ I. Selyuzhenkov,^{96,110} S. Senyukov,¹³⁹ J. J. Seo,⁶³ D. Serebryakov,⁶⁵ L. Šerkšnytė,¹⁰⁸ A. Sevcenco,⁶⁹ T. J. Shaba,⁷⁴ A. Shabanov,⁶⁵ A. Shabetai,¹¹⁷ R. Shahoyan,³⁵ W. Shaikh,¹¹² A. Shangaraev,⁹⁴ A. Sharma,¹⁰³ H. Sharma,¹²⁰ M. Sharma,¹⁰⁴ N. Sharma,¹⁰³ S. Sharma,¹⁰⁴ U. Sharma,¹⁰⁴ O. Sheibani,¹²⁷ K. Shigaki,⁴⁷ M. Shimomura,⁸⁶ S. Shirinkin,⁹⁵ Q. Shou,⁴¹ Y. Sibiriak,⁹¹ S. Siddhanta,⁵⁶ T. Siemiarczuk,⁸⁸ T. F. Silva,¹²³ D. Silvermyr,⁸³ G. Simonetti,³⁵ B. Singh,¹⁰⁸ R. Singh,⁸⁹ R. Singh,¹⁰⁴ R. Singh,⁵¹ V. K. Singh,¹⁴³ V. Singhal,¹⁴³ T. Sinha,¹¹² B. Sitar,¹³ M. Sitta,³² T. B. Skaali,²⁰ G. Skorodumovs,¹⁰⁷ M. Slupecki,⁴⁵ N. Smirnov,¹⁴⁸ R. J. M. Snellings,⁶⁴ C. Soncco,¹¹⁴ J. Song,¹²⁷ A. Songmoolnak,¹¹⁸ F. Soramel,²⁸ S. Sorensen,¹³³ I. Sputowska,¹²⁰ J. Stachel,¹⁰⁷ I. Stan,⁶⁹ P. J. Steffanic,¹³³

S. F. Stiefelmaier,¹⁰⁷ D. Stocco,¹¹⁷ I. Storehaug,²⁰ M. M. Storetvedt,³⁷ C. P. Stylianidis,⁹³ A. A. P. Suaide,¹²³ T. Sugitate,⁴⁷ C. Suire,⁸⁰ M. Sukhanov,⁶⁵ M. Suljic,³⁵ R. Sultanov,⁹⁵ M. Šumbera,⁹⁸ V. Sumberia,¹⁰⁴ S. Sumowidagdo,⁵² S. Swain,⁶⁷ A. Szabo,¹³ I. Szarka,¹³ U. Tabassam,¹⁴ S. F. Taghavi,¹⁰⁸ G. Taillepied,¹³⁷ J. Takahashi,¹²⁴ G. J. Tambave,²¹ S. Tang,^{7,137} Z. Tang,¹³¹ J. D. Tapia Takaki,^{129,g} M. Tarhini,¹¹⁷ M. G. Tarzila,⁴⁹ A. Tauro,³⁵ G. Tejada Muñoz,⁴⁶ A. Telesca,³⁵ L. Terlizzi,²⁵ C. Terrevoli,¹²⁷ G. Tersimonov,³ S. Thakur,¹⁴³ D. Thomas,¹²¹ R. Tieulent,¹³⁸ A. Tikhonov,⁶⁵ A. R. Timmins,¹²⁷ M. Tkacik,¹¹⁹ A. Toia,⁷⁰ N. Topilskaya,⁶⁵ M. Toppi,⁵³ F. Torales-Acosta,¹⁹ T. Tork,⁸⁰ S. R. Torres,³⁸ A. Trifiró,^{33,57} S. Tripathy,^{55,71} T. Tripathy,⁵⁰ S. Trogolo,^{28,35} G. Trombetta,³⁴ V. Trubnikov,³ W. H. Trzaska,¹²⁸ T. P. Trzcinski,¹⁴⁴ B. A. Trzeciak,³⁸ A. Tumkin,¹¹¹ R. Turrisi,⁵⁸ T. S. Tveter,²⁰ K. Ullaland,²¹ A. Uras,¹³⁸ M. Urioni,^{59,142} G. L. Usai,²³ M. Vala,³⁹ N. Valle,^{29,59} S. Vallero,⁶¹ N. van der Kolk,⁶⁴ L. V. R. van Doremalen,⁶⁴ M. van Leeuwen,⁹³ P. Vande Vyvre,³⁵ D. Varga,¹⁴⁷ Z. Varga,¹⁴⁷ M. Varga-Kofarago,¹⁴⁷ A. Vargas,⁴⁶ M. Vasileiou,⁸⁷ A. Vasiliev,⁹¹ O. Vázquez Doce,^{53,108} V. Vechernin,¹¹⁵ E. Vercellin,²⁵ S. Vergara Limón,⁴⁶ L. Vermunt,⁶⁴ R. Vértesi,¹⁴⁷ M. Verweij,⁶⁴ L. Vickovic,³⁶ Z. Vilakazi,¹³⁴ O. Villalobos Baillie,¹¹³ G. Vino,⁵⁴ A. Vinogradov,⁹¹ T. Virgili,³⁰ V. Vislavicius,⁹² A. Vodopyanov,⁷⁷ B. Volkel,³⁵ M. A. Völkl,¹⁰⁷ K. Voloshin,⁹⁵ S. A. Voloshin,¹⁴⁵ G. Volpe,³⁴ B. von Haller,³⁵ I. Vorobyev,¹⁰⁸ D. Voscek,¹¹⁹ N. Vozniuk,⁶⁵ J. Vrláková,³⁹ B. Wagner,²¹ C. Wang,⁴¹ D. Wang,⁴¹ M. Weber,¹¹⁶ R. J. G. V. Weelden,⁹³ A. Wegrzynek,³⁵ S. C. Wenzel,³⁵ J. P. Wessels,¹⁴⁶ J. Wiechula,⁷⁰ J. Wikne,²⁰ G. Wilk,⁸⁸ J. Wilkinson,¹¹⁰ G. A. Willems,¹⁴⁶ B. Windelband,¹⁰⁷ M. Winn,¹⁴⁰ W. E. Witt,¹³³ J. R. Wright,¹²¹ W. Wu,⁴¹ Y. Wu,¹³¹ R. Xu,⁷ A. K. Yadav,¹⁴³ S. Yalcin,⁷⁹ Y. Yamaguchi,⁴⁷ K. Yamakawa,⁴⁷ S. Yang,²¹ S. Yano,⁴⁷ Z. Yin,⁷ H. Yokoyama,⁶⁴ I.-K. Yoo,¹⁷ J. H. Yoon,⁶³ S. Yuan,²¹ A. Yuncu,¹⁰⁷ V. Zaccolo,²⁴ C. Zampolli,³⁵ H. J. C. Zanolli,⁶⁴ N. Zardoshti,³⁵ A. Zarochentsev,¹¹⁵ P. Závada,⁶⁸ N. Zaviyalov,¹¹¹ M. Zhalov,¹⁰¹ B. Zhang,⁷ S. Zhang,⁴¹ X. Zhang,⁷ Y. Zhang,¹³¹ V. Zhrebchevskii,¹¹⁵ Y. Zhi,¹¹ N. Zhigareva,⁹⁵ D. Zhou,⁷ Y. Zhou,⁹² J. Zhu,^{7,110} Y. Zhu,⁷ A. Zichichi,²⁶ G. Zinovjev,³ and N. Zurlo^{59,142}

A Large Ion Collider Experiment Collaboration

¹A.I. Alikhanyan National Science Laboratory (Yerevan Physics Institute) Foundation, Yerevan, Armenia

²AGH University of Science and Technology, Cracow, Poland

³Bogolyubov Institute for Theoretical Physics, National Academy of Sciences of Ukraine, Kiev, Ukraine

⁴Bose Institute, Department of Physics and Centre for Astroparticle Physics and Space Science (CAPSS), Kolkata, India

⁵Budker Institute for Nuclear Physics, Novosibirsk, Russia

⁶California Polytechnic State University, San Luis Obispo, California, United States

⁷Central China Normal University, Wuhan, China

⁸Centro de Aplicaciones Tecnológicas y Desarrollo Nuclear (CEADEN), Havana, Cuba

⁹Centro de Investigación y de Estudios Avanzados (CINVESTAV), Mexico City and Mérida, Mexico

¹⁰Chicago State University, Chicago, Illinois, United States

¹¹China Institute of Atomic Energy, Beijing, China

¹²Chungbuk National University, Cheongju, Republic of Korea

¹³Comenius University Bratislava, Faculty of Mathematics, Physics and Informatics, Bratislava, Slovakia

¹⁴COMSATS University Islamabad, Islamabad, Pakistan

¹⁵Creighton University, Omaha, Nebraska, United States

¹⁶Department of Physics, Aligarh Muslim University, Aligarh, India

¹⁷Department of Physics, Pusan National University, Pusan, Republic of Korea

¹⁸Department of Physics, Sejong University, Seoul, Republic of Korea

¹⁹Department of Physics, University of California, Berkeley, California, United States

²⁰Department of Physics, University of Oslo, Oslo, Norway

²¹Department of Physics and Technology, University of Bergen, Bergen, Norway

²²Dipartimento di Fisica dell'Università "La Sapienza" and Sezione INFN, Rome, Italy

²³Dipartimento di Fisica dell'Università and Sezione INFN, Cagliari, Italy

²⁴Dipartimento di Fisica dell'Università and Sezione INFN, Trieste, Italy

²⁵Dipartimento di Fisica dell'Università and Sezione INFN, Turin, Italy

²⁶Dipartimento di Fisica e Astronomia dell'Università and Sezione INFN, Bologna, Italy

²⁷Dipartimento di Fisica e Astronomia dell'Università and Sezione INFN, Catania, Italy

²⁸Dipartimento di Fisica e Astronomia dell'Università and Sezione INFN, Padova, Italy

²⁹Dipartimento di Fisica e Nucleare e Teorica, Università di Pavia, Pavia, Italy

³⁰Dipartimento di Fisica "E.R. Caianiello" dell'Università and Gruppo Collegato INFN, Salerno, Italy

³¹Dipartimento DISAT del Politecnico and Sezione INFN, Turin, Italy

- ³²*Dipartimento di Scienze e Innovazione Tecnologica dell'Università del Piemonte Orientale and INFN Sezione di Torino, Alessandria, Italy*
- ³³*Dipartimento di Scienze MIFT, Università di Messina, Messina, Italy*
- ³⁴*Dipartimento Interateneo di Fisica "M. Merlin" and Sezione INFN, Bari, Italy*
- ³⁵*European Organization for Nuclear Research (CERN), Geneva, Switzerland*
- ³⁶*Faculty of Electrical Engineering, Mechanical Engineering and Naval Architecture, University of Split, Split, Croatia*
- ³⁷*Faculty of Engineering and Science, Western Norway University of Applied Sciences, Bergen, Norway*
- ³⁸*Faculty of Nuclear Sciences and Physical Engineering, Czech Technical University in Prague, Prague, Czech Republic*
- ³⁹*Faculty of Science, P.J. Šafárik University, Košice, Slovakia*
- ⁴⁰*Frankfurt Institute for Advanced Studies, Johann Wolfgang Goethe-Universität Frankfurt, Frankfurt, Germany*
- ⁴¹*Fudan University, Shanghai, China*
- ⁴²*Gangneung-Wonju National University, Gangneung, Republic of Korea*
- ⁴³*Gauhati University, Department of Physics, Guwahati, India*
- ⁴⁴*Helmholtz-Institut für Strahlen- und Kernphysik, Rheinische Friedrich-Wilhelms-Universität Bonn, Bonn, Germany*
- ⁴⁵*Helsinki Institute of Physics (HIP), Helsinki, Finland*
- ⁴⁶*High Energy Physics Group, Universidad Autónoma de Puebla, Puebla, Mexico*
- ⁴⁷*Hiroshima University, Hiroshima, Japan*
- ⁴⁸*Hochschule Worms, Zentrum für Technologietransfer und Telekommunikation (ZTT), Worms, Germany*
- ⁴⁹*Horia Hulubei National Institute of Physics and Nuclear Engineering, Bucharest, Romania*
- ⁵⁰*Indian Institute of Technology Bombay (IIT), Mumbai, India*
- ⁵¹*Indian Institute of Technology Indore, Indore, India*
- ⁵²*Indonesian Institute of Sciences, Jakarta, Indonesia*
- ⁵³*INFN, Laboratori Nazionali di Frascati, Frascati, Italy*
- ⁵⁴*INFN, Sezione di Bari, Bari, Italy*
- ⁵⁵*INFN, Sezione di Bologna, Bologna, Italy*
- ⁵⁶*INFN, Sezione di Cagliari, Cagliari, Italy*
- ⁵⁷*INFN, Sezione di Catania, Catania, Italy*
- ⁵⁸*INFN, Sezione di Padova, Padova, Italy*
- ⁵⁹*INFN, Sezione di Pavia, Pavia, Italy*
- ⁶⁰*INFN, Sezione di Roma, Rome, Italy*
- ⁶¹*INFN, Sezione di Torino, Turin, Italy*
- ⁶²*INFN, Sezione di Trieste, Trieste, Italy*
- ⁶³*Inha University, Incheon, Republic of Korea*
- ⁶⁴*Institute for Gravitational and Subatomic Physics (GRASP), Utrecht University/Nikhef, Utrecht, Netherlands*
- ⁶⁵*Institute for Nuclear Research, Academy of Sciences, Moscow, Russia*
- ⁶⁶*Institute of Experimental Physics, Slovak Academy of Sciences, Košice, Slovakia*
- ⁶⁷*Institute of Physics, Homi Bhabha National Institute, Bhubaneswar, India*
- ⁶⁸*Institute of Physics of the Czech Academy of Sciences, Prague, Czech Republic*
- ⁶⁹*Institute of Space Science (ISS), Bucharest, Romania*
- ⁷⁰*Institut für Kernphysik, Johann Wolfgang Goethe-Universität Frankfurt, Frankfurt, Germany*
- ⁷¹*Instituto de Ciencias Nucleares, Universidad Nacional Autónoma de México, Mexico City, Mexico*
- ⁷²*Instituto de Física, Universidade Federal do Rio Grande do Sul (UFRGS), Porto Alegre, Brazil*
- ⁷³*Instituto de Física, Universidad Nacional Autónoma de México, Mexico City, Mexico*
- ⁷⁴*iThemba LABS, National Research Foundation, Somerset West, South Africa*
- ⁷⁵*Jeonbuk National University, Jeonju, Republic of Korea*
- ⁷⁶*Johann-Wolfgang-Goethe Universität Frankfurt Institut für Informatik, Fachbereich Informatik und Mathematik, Frankfurt, Germany*
- ⁷⁷*Joint Institute for Nuclear Research (JINR), Dubna, Russia*
- ⁷⁸*Korea Institute of Science and Technology Information, Daejeon, Republic of Korea*
- ⁷⁹*KTO Karatay University, Konya, Turkey*
- ⁸⁰*Laboratoire de Physique des 2 Infinis, Irène Joliot-Curie, Orsay, France*
- ⁸¹*Laboratoire de Physique Subatomique et de Cosmologie, Université Grenoble-Alpes, CNRS-IN2P3, Grenoble, France*
- ⁸²*Lawrence Berkeley National Laboratory, Berkeley, California, United States*
- ⁸³*Lund University Department of Physics, Division of Particle Physics, Lund, Sweden*
- ⁸⁴*Moscow Institute for Physics and Technology, Moscow, Russia*
- ⁸⁵*Nagasaki Institute of Applied Science, Nagasaki, Japan*
- ⁸⁶*Nara Women's University (NWU), Nara, Japan*
- ⁸⁷*National and Kapodistrian University of Athens, School of Science, Department of Physics, Athens, Greece*
- ⁸⁸*National Centre for Nuclear Research, Warsaw, Poland*
- ⁸⁹*National Institute of Science Education and Research, Homi Bhabha National Institute, Jatni, India*
- ⁹⁰*National Nuclear Research Center, Baku, Azerbaijan*

- ⁹¹National Research Centre Kurchatov Institute, Moscow, Russia
⁹²Niels Bohr Institute, University of Copenhagen, Copenhagen, Denmark
⁹³Nikhef, National institute for subatomic physics, Amsterdam, Netherlands
⁹⁴NRC Kurchatov Institute IHEP, Protvino, Russia
⁹⁵NRC Kurchatov Institute IHEP, Moscow, Russia
⁹⁶NRNU Moscow Engineering Physics Institute, Moscow, Russia
⁹⁷Nuclear Physics Group, STFC Daresbury Laboratory, Daresbury, United Kingdom
⁹⁸Nuclear Physics Institute of the Czech Academy of Sciences, Řež u Prahy, Czech Republic
⁹⁹Oak Ridge National Laboratory, Oak Ridge, Tennessee, United States
¹⁰⁰Ohio State University, Columbus, Ohio, United States
¹⁰¹Petersburg Nuclear Physics Institute, Gatchina, Russia
¹⁰²Physics department, Faculty of science, University of Zagreb, Zagreb, Croatia
¹⁰³Physics Department, Panjab University, Chandigarh, India
¹⁰⁴Physics Department, University of Jammu, Jammu, India
¹⁰⁵Physics Department, University of Rajasthan, Jaipur, India
¹⁰⁶Physikalisches Institut, Eberhard-Karls-Universität Tübingen, Tübingen, Germany
¹⁰⁷Physikalisches Institut, Ruprecht-Karls-Universität Heidelberg, Heidelberg, Germany
¹⁰⁸Physik Department, Technische Universität München, Munich, Germany
¹⁰⁹Politecnico di Bari and Sezione INFN, Bari, Italy
¹¹⁰Research Division and ExtreMe Matter Institute EMMI, GSI Helmholtzzentrum für Schwerionenforschung GmbH, Darmstadt, Germany
¹¹¹Russian Federal Nuclear Center (VNIIEF), Sarov, Russia
¹¹²Saha Institute of Nuclear Physics, Homi Bhabha National Institute, Kolkata, India
¹¹³School of Physics and Astronomy, University of Birmingham, Birmingham, United Kingdom
¹¹⁴Sección Física, Departamento de Ciencias, Pontificia Universidad Católica del Perú, Lima, Peru
¹¹⁵St. Petersburg State University, St. Petersburg, Russia
¹¹⁶Stefan Meyer Institut für Subatomare Physik (SMI), Vienna, Austria
¹¹⁷SUBATECH, IMT Atlantique, Université de Nantes, CNRS-IN2P3, Nantes, France
¹¹⁸Suranaree University of Technology, Nakhon Ratchasima, Thailand
¹¹⁹Technical University of Košice, Košice, Slovakia
¹²⁰The Henryk Niewodniczanski Institute of Nuclear Physics, Polish Academy of Sciences, Cracow, Poland
¹²¹The University of Texas at Austin, Austin, Texas, United States
¹²²Universidad Autónoma de Sinaloa, Culiacán, Mexico
¹²³Universidade de São Paulo (USP), São Paulo, Brazil
¹²⁴Universidade Estadual de Campinas (UNICAMP), Campinas, Brazil
¹²⁵Universidade Federal do ABC, Santo Andre, Brazil
¹²⁶University of Cape Town, Cape Town, South Africa
¹²⁷University of Houston, Houston, Texas, United States
¹²⁸University of Jyväskylä, Jyväskylä, Finland
¹²⁹University of Kansas, Lawrence, Kansas, United States
¹³⁰University of Liverpool, Liverpool, United Kingdom
¹³¹University of Science and Technology of China, Hefei, China
¹³²University of South-Eastern Norway, Tonsberg, Norway
¹³³University of Tennessee, Knoxville, Tennessee, United States
¹³⁴University of the Witwatersrand, Johannesburg, South Africa
¹³⁵University of Tokyo, Tokyo, Japan
¹³⁶University of Tsukuba, Tsukuba, Japan
¹³⁷Université Clermont Auvergne, CNRS/IN2P3, LPC, Clermont-Ferrand, France
¹³⁸Université de Lyon, CNRS/IN2P3, Institut de Physique des 2 Infinis de Lyon, Lyon, France
¹³⁹Université de Strasbourg, CNRS, IPHC UMR 7178, F-67000 Strasbourg, France, Strasbourg, France
¹⁴⁰Université Paris-Saclay Centre d'Etudes de Saclay (CEA), IRFU, Département de Physique Nucléaire (DPHn), Saclay, France
¹⁴¹Università degli Studi di Foggia, Foggia, Italy
¹⁴²Università di Brescia, Brescia, Italy
¹⁴³Variable Energy Cyclotron Centre, Homi Bhabha National Institute, Kolkata, India
¹⁴⁴Warsaw University of Technology, Warsaw, Poland
¹⁴⁵Wayne State University, Detroit, Michigan, United States
¹⁴⁶Westfälische Wilhelms-Universität Münster, Institut für Kernphysik, Münster, Germany
¹⁴⁷Wigner Research Centre for Physics, Budapest, Hungary
¹⁴⁸Yale University, New Haven, Connecticut, United States
¹⁴⁹Yonsei University, Seoul, Republic of Korea

^aDeceased.

^bAlso at Dipartimento DET del Politecnico di Torino, Turin, Italy.

^cAlso at M.V. Lomonosov Moscow State University, D.V. Skobeltsyn Institute of Nuclear Physics, Moscow, Russia.

^dAlso at Department of Applied Physics, Aligarh Muslim University, Aligarh, India.

^eAlso at Institute of Theoretical Physics, University of Wrocław, Poland.

^fAlso at University of Kansas, Lawrence, Kansas, United States.

^gAlso at Italian National Agency for New Technologies, Energy and Sustainable Economic Development (ENEA), Bologna, Italy.